Eka Suarso _ Enhancement of LiFePO4 (LFP) electrochemical performance through the insertion of coconut shellderived rGO-like carbon as cathode of Li-ion battery

by Iqbal Syaichurrozi

Submission date: 28-Nov-2024 07:11AM (UTC+0700)
Submission ID: 2456862391
File name: rso,_2021_Enhancement_of_LiFePO4_LFP_electrochemical_perform.pdf (1.26M)
Word count: 6281
Character count: 32584

J Mater Sci: Mater Electron (2021) 32:28297–28306

Enhancement of $LiFePO_4$ (LFP) electrochemical performance through the insertion of coconut shell-derived rGO-like carbon as cathode of Li-ion battery

E. Suarso[1,2], F. A. Setyawan[1], A. Subhan[3], M. Mahyiddin Ramli[4], N. Syakimah Ismail[4], M. Zainuri[1], Z. Arifin[1], and Darminto[1,*]

[1] Advanced Materials Research Group, Department of Physics, Insitut Teknologi Sepuluh Nopember, Campus of ITS Sukolilo, Surabaya 60111, Indonesia

[2] Physics Study Program, Faculty of Mathematics and Natural Sciences, Universitas Lambung Mangkurat Jl., Ahmad Yani Km 36,00, Banjarbaru, Kalimantan Selatan 70714, Indonesia

[3] Research Center for Physics, Indonesian Institute of Sciences (LIPI), Serpong, Tangerang Selatan 15314, Indonesia

[4] School of Microelectronic Engineering, Universiti Malaysia Perlis, Pauh Putra Campus, 02600 Arau, Perlis, Malaysia

Received: 4 March 2021
Accepted: 9 October 2021
Published online: 21 October 2021

ABSTRACT

An old coconut shell as a green biomass was known as a potential carbon materials for rGO and cost effectiveness. The objective of this study is synthesizing an rGO-like carbon (C) compound from coconut shells and inserting into $LiFePO_4$ (LFP), as Li-ion battery cathode. Thus, an LFP/rGO nanocomposite was successfully fabricated using an unconventional approach which is the combination of the sol–gel technique and mechanical ultracentrifugation. $LiFePO_4$ precursors were prepared from commercial starting materials, using the sol–gel technique, and the composites' carbon weight content was varied between 15 and 30%. This process was subsequently followed by evaluating the microstructural characteristics and electrochemical properties as cathode for the Li-ion batteries. The results showed a high tendency of achieving maximum efficiency with merged LFP and rGO, although LFP molecules appear scattered but are firmly attached to each rGO structure, acting as a "bridge" between the surrounding particles. This reduced graphene oxide (rGO) link is relatively effective in limiting LFP grain growth as well as expanding the surface area, leading to a decline in Li-ion diffusion rate. Consequently, the bridge presence also demonstrated a significant effect by enhancing the conductivity, electrical capacity, and performance of the LFP/rGO cycle than pure LFP. Furthermore, the percentage ratio of the synthesized LFP/rGO cathode (85:15) attained higher cycle capacity, compared to 70:30 on the level of 0.1 C, with specific discharging average of 128.03 $mAhg^{-1}$ and retention capacity of 97.75% after 50 cycles, at room temperature and a rate of 0.1 C.

Address correspondence to E-mail: darminto@physics.its.ac.id

https://doi.org/10.1007/s10854-021-07206-5

1 Introduction

Lithium iron phosphate (LFP) was firstly reported in 1997, by Goodenough *et al.*, became a promising cathode material for rechargeable Li-ion batteries, and has long been studied intensively afterward [1, 2]. This is due to the easy to obtain, non-toxic, environmentally friendly, and cheaply manufactured constituent materials [2–4]. In addition, LFP with olivine structure ($LiFePO_4$) shows a high theoretical capacity (170 $mAhg^{-1}$), operating voltage suitable (3.5V vs Li^+/Li), long life, and high thermal stability [3, 4]. However, limitation of lithium ions such as low intrinsic electronic conductivity and slow diffusion rate for the application in Li-ion batteries are particularly at low temperatures and high current densities [3, 5]. Therefore, a combination of carbon bridging and particle size reduction is one of the most effective strategies to overcome this problem [2, 5, 6]. This carbon bridging effort aims to inhibit crystal growth [7, 8], blocking particle agglomeration [4, 9], strengthen contact inter-particles [10], and shorten the lithium ion diffusion pathways [11, 12], while the presence of a carbon layer prevents Fe^{2+} oxidization to Fe^{3+}; thus, the material's purity is guaranteed [12].

Coconut shells have been studied as a potential carbon materials for rGO [13, 14] with advantages not only in the green energy issue but also in the cheaper cost compared to the commercial ones [15]. Carbon material is one of the optimal selection of the electrode material [16]. Recent studies showed that carbon-based integrations, including carbon nanotubes (CNT) or graphene, accelerate the movement of photo-generated electrons and generate easier charge separations [17] while enhancing the thermoelectric characteristics [18]. Graphene exhibits exceptional electron transport properties and very substantial carrier-mobility [19]. In terms of electrical conductivity, the substance demonstrates high capacity to increase power conversion efficiency [20] and its stability [21]. Moreover, graphene as a carbon-based nanocomposite advantages are mostly on the economic concern and the environmental impact [22]. Reduced graphene oxide (rGO), as part of Graphene-based nanomaterials, is having particular interest among the various activated carbon materials available due to its high electronic conductivity, wide surface area, structural flexibility, chemical stability, wide operating temperature range, and unique characteristics of a single atomic thick layer [23–25]. Furthermore, rGO is a major functional graphene derivative formed from the graphene oxide reduction process that involves the addition of electrons to an atom or atomic network [26]. Based on the unique structure and excellent characteristics, the nanocomposite also occurs among the most promising materials for possible application in lithium ion battery electrodes [23, 27, 28]. Recently, graphene and its derivatives, including rGO-based samples, have been analyzed extensively after demonstrating significantly enhanced electrochemical performance and stability [29, 30].

The preparation of LFP/rGO nanocomposites does not only tend to improve the cathode material's conductivity but also shortens the lithium ions' diffusion path and increasing the lithium ion diffusion rate and then improving the material's electrochemical performance [31]. During the last decade, research on bridging LFP cathode material with graphene and its derivatives, such as rGO in composite form, were conducted [3, 23]. Shang *et al.* synthesized a LFP/graphene composite by the liquid phase method that showed an initial specific discharge capacity of 160 $mAhg^{-1}$ at 0.1 C [32]. Meanwhile, Yuan *et al.* synthesized a $LiFePO_4$/rGO composite through a simple solid phase combined with a carbothermal reduction method that resulted a first special discharge capacity of 151.5 $mAhg^{-1}$ at 0.1 C, and 149.2 $mAhg^{-1}$ after 50 cycles, with a coulombic efficiency of 98.5% [33]. Furthermore, Dhindsa *et al.* synthesized $LiFePO_4$/graphene nanocomposites by the sol–gel method and the constant current test results showed that $LiFePO_4$/G composite had a higher initial discharge capacity at a 0.1 C current density, compared to pure $LiFePO_4$ [34]. Similarly, Yuan et al. successfully prepared rGO composites based on $LiFePO_4$ using the hydrothermal method [35], and almost all the result indicated better electrochemical performance and stability in the composites and LFP/graphene composites have also been successfully prepared through in situ solvothermal methods [36, 37], solid-state reaction [38, 39], and co-precipitation method [40]. Generally, the composites produced from these various synthesis methods are significantly improving the $LiFePO_4$ electrode's electrochemical performance [35]. In terms of simplicity, manufacturing of $LiFePO_4$ nanocomposites in order to control $LiFePO_4$'s morphology is more preferable since nanocomposites are made by simply mixing components and

conductivity controllable by carefully selecting its components [29, 39, 41]. However, certain mechanisms employ expensive and environmentally unfriendly commercial chemicals in LFP/graphene nanocomposites, with a complex manufacturing process. Therefore, further research that utilizes low cost and sustainable (green) materials through a new and simpler approach appears very necessary [26, 42–45].

Previously [41], preparation method of LFP/rGO nanocomposites is using polymerized Polypyrrole in situ and [7] is using limited precipitation polymerization in situ at room temperature. Nano-structured LiFePO4 particles and rGO potentials are believed to be suitable candidates for further developing of cathode materials for lithium-ion batteries. In this study, an old coconut shell waste (biomass) was used to prepare an rGO-like carbon, as a "green" (sustainable) compound, acting as material for technological applications in the form of high-performance cathode materials for lithium ion batteries. The aim of this study is to provide an overview on old coconut shell (biomass) utilization to generate rGO as a sustainable compound in battery technology. As a consequence, a novel approach was introduced to evaluate the microstructural characteristics and electrochemical properties of rGO-based LFP cathodes. Specifically, the research scope covers the following: (i) obtaining a close relationship between the LFP and rGO substances needed for maximum efficiency; (ii) providing vital ideas related to natural resource utilization, including coconut shells (biomass), used to prepare the rGO-like carbon as a "green" (sustainable) compound in technological applications in form of high-performance cathode materials for lithium ion batteries; and (iii) developing an efficient method to synthesize functional LFP/rGO nanocomposites as superior lithium ion battery cathode materials, compared to previous studies [7, 41]. A combination of sol–gel and mechanical ultracentrifugation techniques with emphasis on super high centrifugation speed is required.

2 Method

The material preparation is particular focused on $LiFePO_4$ and rGO composites. During $LiFePO_4$ nanoparticles preparation, firstly, the $LiFePO_4$ nanoparticles were prepared by sol–gel approach using Li_2CO_3, $FeCl_2{\cdot}4H_2O$, and $NH_4H_2PO_4$ powders as precursors. Secondly, the materials were mixed and homogenized using a magnetic stirrer into a solution. Thirdly, the resulted sol solution was slowly dripped with NH_4OH until a pH of 7 was obtained, while continuously stirred and heated at 100 °C for 3 h until a gel was formed. Finally, the precursor gel was dried at 120 °C, and further heating at 700 °C and 750 °C in an argon gas environment for 10 h at 5 °C/s resulted in xerogel and calcinated substances, respectively. Meanwhile, in rGO preparation, the first step is rGO-like carbon compound was synthesized from old coconut shells, subjected to be burning, pulverizing as well as sieving. The second step is the obtained charcoal powder was carbonized in a furnace at 400 °C for 5 h. At third step, a mechanical and chemical exfoliating process using HCl was carried out for 6 h to unbond rGO layers and resulting thinner particle size.

Furthermore, the LFP/rGO nanocomposite cathode was prepared by mechanical ultracentrifugation approach. This was performed by adding the rGO solution into $LiFePO_4$ nanoparticles and mixed with normal butanol (N-butanol). The mixture was dispensed and stirred with a magnetic stirrer at 120 °C for 5 h. The resulting sample was then ultrasonised until the rGO layers were estimated to be covering the LPF particles and subjected to be polarized. Subsequently, the newly formed LFP/rGO slurry was centrifuged at 6000 rpm for 40 min to generate a LFP/rGO nanocomposite structure, prior to drying at 80 °C for 2 h. This process is believed to serve as an advancement of the previous method [46].

The crystal structure, phase composition, and lattice parameters of LFP nanoparticles as well as the rGO composites were characterized using the Philips X'Pert MPD X-Ray diffraction instrument (multipurpose diffractometer) and Cu Kα (λ = 1.54060 Å) radiation. Also, the rGO occurrence was determined by Raman spectroscopy (Raman spectrometer—Renishaw InVia), while the transmission electron microscope (TEM, Tecnai G2-200 keV, Philips) was used to observe the morphology and microstructure. In addition, the morphology and crystal size were examined by scanning electron microscopy (SEM-EDX, ZEISS).

The $LiFePO_4$-based nanocomposite cathode's electrochemical properties were measured using a CR2016 coin cell, with a lithium metal disc as the electrode counter. Meanwhile, the working electrodes

were assembled by pressing a mixture of the synthesized $LiFePO_4$/rGO, polyvinylidene fluoride (PVDF) binder, and super-p addictive material, in a 0.5:0.033:0.022 weight ratio. The electrolyte was created from 1M $LiPF_6$ dissolved in a mixture of ethylene carbonate (EC) and dimethyl carbonate (DMC) (1:1:1, v/v/v) as well as Li-foil and Celgard 2300 microfilm used as separator and counter electrode. Furthermore, the coin cells were assembled in a glove box filled with high-purity Ar gas, while the $LiFePO_4$/rGO electrical conductivity test was conducted with a four-point probe. The galvanostatic charge/discharge is tested in the voltage range of 0.5–4.0 V vs Li/Li^+ at various current levels, while electrochemical impedance spectroscopy (EIS) and cyclic voltammetry (CV) were measured above the CHI-660D electrochemical workstation, at 0.1 mVs^{-1} in 0.5–2.1 V vs $Zn°/Zn^{2+}$. EIS measurements were performed over the frequency range of 0.01 Hz–100 kHz at the discharge stage, with 5 mV amplitude.

3 Results and discussion

Figure 1 shows the X-ray diffraction (XRD) patterns revealed by the two LFP sample structure shapes and phase purities. Based on phase identification from the XRD pattern results, the two LFP sample's crystalinity were analyzed. Both patterns show similar $LiFePO_4$ main diffraction peaks and match the orthorhombic structure as well as Pnma space group. The sharp, narrow diffraction peaks without detectable phase impurities indicate that the LFP sample has high crystalinity. For the sample calcined at 750 °C, an olivine phase without detectable impurity phases was observed, while the 700 °C sample showed a 97% pure olivine phase and a phase impurity in the form of $FeO_{11}P_4$. The LFP sample calcined at 750 °C had a sharper diffraction peak with narrower full width at half maximum (FWHM) and a higher intensity, compared to the 700 °C counterpart. According to the peak FWHM, the crystal size of the samples prepared at 700 °C and 750 °C calculated by the Scherrer equation resulted in 99 nm and 100 nm, respectively.

Figure 2 shows the XRD spectrum and Raman shift curve of coconut shell-based rGO after furnace carbonization for 5 hours at 400 °C. Based on the illustration, the rGO phase was observed by the presence of two broad peaks at positions 23.5° and 42.5° along the 002 and 100 planes, respectively. Similarly, two main crests with wavenumbers 1370 cm^{-1} (band D) and 1620 cm^{-1} (band G) were also recorded. The defect band (D) was caused by crystal defects during synthesis, while the graphite band (G) represented the graphite bonds shared by the entire carbon allotropes, including graphite, graphene, activated carbon, and carbon nanotubes (CNT). In pure graphene,

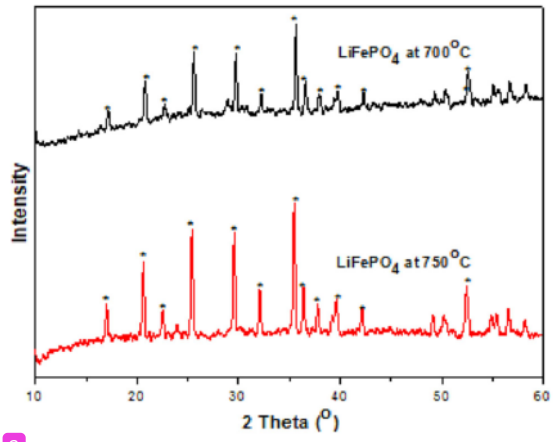

Fig. 1 XRD patterns of LFP preparation at temperatures of 700 °C and 750 °C

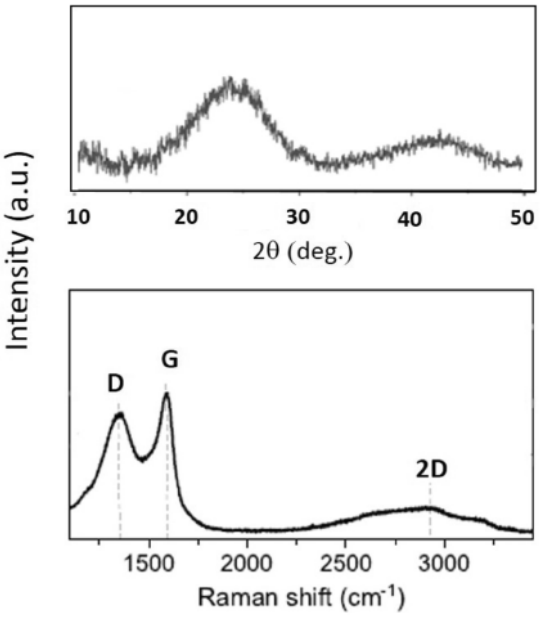

Fig. 2 The XRD spectrum and Raman shift curve of rGO based on coconut shell

the crystal structure is dominated by single-dimensional hexagonal carbon bonds, indicating a perfect state and low-intensity D band. This condition is validated by calculating the I_D/I_G ratio that represents the proportional value of the intensities of the defect (D) to graphene (G). Based on the relationship, greater I_D/I_G estimates tend to increase the defects, resulting in a weak hexagonal bonding in graphene sheet that possibly confirms an rGO phase. Meanwhile, the broad peak in 2D band shows the number of layers that are subsequently formed. Figure 3 represents the transmission electron microscopy (TEM) images of rGO samples. The TEM results revealed the occurrence of several aggregated layers that are individually stacked, although with slight wrinkles and transparency, due to the reduction process.

The LFP/rGO nanocomposite particles' morphological and microstructure are observable with SEM–EDX (Fig. 4). Based on the images, LFP particles have spherical lumps and are firmly attached to rGO, resembling a thin flake (Fig. 4a and b). LFP's spherical lumps indicate agglomeration, where several particles are joined together to look larger, with a non-homogenous and unevenly distributed grain size in certain places. This agglomeration occurs since the LFP powder, rGO solution, and N-butanol are not evenly mixed in the slurry-making process, while the black lumps indicate that the cathode sheet has shafts. Figure 4b shows that large LFP particles are scattered and firmly attached to each rGO layer side, thus acting as a "bridge" among the particles surroundings. Lithium ion has a greater diffusion distance between the crystal grain's boundary and center due to the larger crystal size. Furthermore, the rGO bridge is quite effective in limiting the LFP's grain growth and widening the surface area, shortening the lithium ion's diffusion length. Therefore, the close relationship between LFP and rGO nanoparticles encourages maximum efficiency while implementing the framework. The presence of Fe, P, O, and C were confirmed in EDX elemental analysis for the LFP/rGO nanocomposite at Fig. 4c. The graph showed various colors of the element mapping, including Fe (pink) on the energy position 0.65 keV and 6.40 keV, P (blue) at 2.0 keV, and O (green) at 0.46 keV that formed the violet color and was assumed as LFP nanoparticle. Meanwhile, C element represented rGO with red color on the energy position of 0.24 keV and K element (light blue) was also founded in the sample. Furthermore, the raw atomic ratios were C, O, Fe, P, and K with 41.93%, 35.41%, 13.98%, 8.46%, and 0.22%, respectively (Table 1). This EDX element mapping approach also can be found in [8, 47].

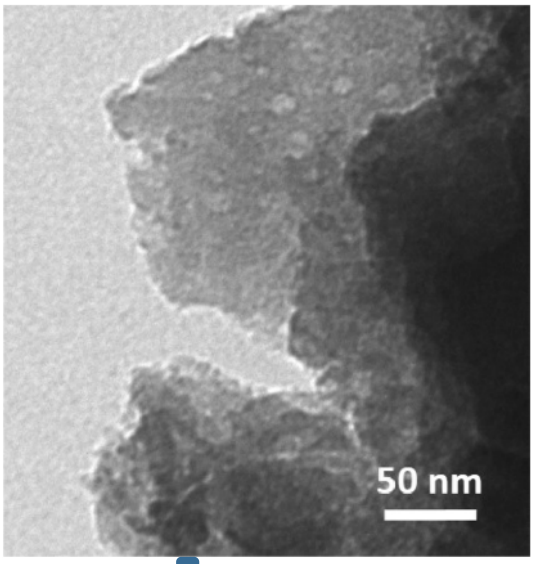

Fig. 3 TEM image of reduced graphene oxide (rGO) based on old coconut shell

Figure 5 shows the LFP/rGO nanocomposites' electronic conductivity and stored energy that are much higher, compared to pure LFP. Mixing $LiFePO_4$ particles with rGO by mechanical ultracentrifugation plays a significant role in enhancing the electronic conductivity and stored energy. These properties increase with the raise in rGO percentage. The optimum result of 7.84×10^{-4} S/cm was obtained for samples with a mass ratio of 70% LFP and 30% rGO, while the counterparts for pure $LiFePO_4$ (theoretical) and LFP synthesized by the sol–gel method are $\sim 10^{-9}$ S/cm and 2.09×10^{-7} S/cm, respectively.

Meanwhile, energy stored from LFP/rGO nanocomposites show a unique phenomenon and the optimum value of 6.50×10^{-3} J was obtained by samples with a mass ratio of 85% LFP and 15% rGO. This explains that the addition of rGO bridging LFP particles must be carried out within certain limits and is reinforced by the LFP/rGO nanocomposite cathode material's electrochemical properties. A lithium battery's energy capacity depends on how many lithium ions are stored in the electrode structure and how much the ions are able to move during charging

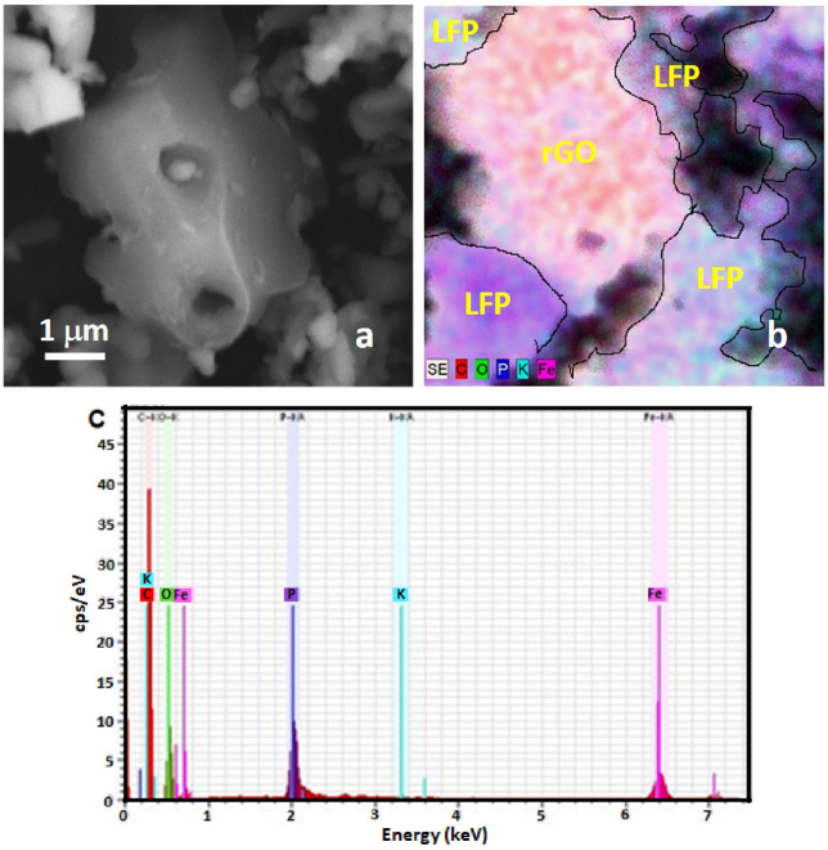

Fig. 4 Images of **a** SEM, **b** the elemental mapping, and **c** EDX spectrum for LFP/rGO nanocomposite

Table 1 The LFP/rGO nanocomposite particles EDX elements analysis

Element	Atomic number (AN)	Series	Wt (%)
C	6	K-series	41.93
O	8	K-series	35.41
Fe	26	K-series	13.98
P	15	K-series	8.46
K	19	K-series	0.22
Total			100.00

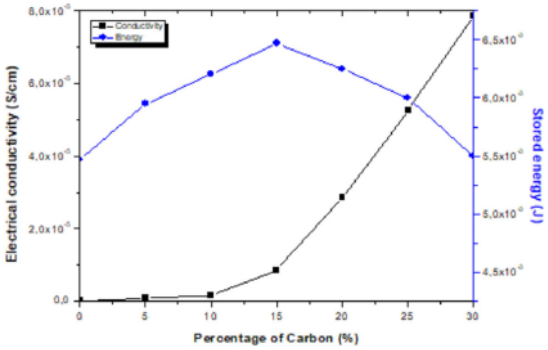

Fig. 5 Electrical conductivity and stored energy vs carbon additions in the LFP/rGO nanocomposite

and discharging due to the amount of electron current stored and distributed is proportional to the amount of lithium ions diffused. Further discussion is to refer to the two samples, for a comparative study.

Figure 6 shows the LFP/rGO nanocomposite's cyclic voltammogram curve with the addition of 15% and 30% rGO percentages in the first charge–discharge cycle [48]. Both curves show sharp and symmetric anodic/cathodic peaks, indicating good electrochemical performance due to single electron transfer reaction during the cycle. In addition, both electrodes showed a Fe^{2+}/Fe^{3+} redox peak at a

0.1 mVs^{-1} scan rate. In the meantime, for LFP/rGO nanocomposites with a 85–15% mass ratio, the peak anodic was located at 3.46 V and corresponds to the oxidation of Fe^{2+} to Fe^{3+} though the cathodic peak at 3.30 V corresponds to the reduction of Fe^{3+} to Fe^{2+} with a 0.16 V potential interval between the two redox peaks. The anodic and cathodic peaks' voltage difference within the same cycle correlates to the redox reaction's polarization and inverse indicating the battery material's reversibility. A reduction in voltage difference lowers the polarization and increases the battery material's reversibility, resulting in greater cycle stability, so consistent with the charge–discharge graph and accelerates the Li^+ ions' diffusion rate. The observed separation between the oxidation and reduction peaks is often used to distinguish electrochemical reversibility from electrode materials with larger separations which indicates lower reversibility. This narrow separation from the redox peak implies that the LFP/rGO nanocomposite has excellent electrochemical kinetics.

Figure 7 shows the Nyquist plot derived from the electrochemical impedance spectroscopies (EIS) of both LFP/rGO nanocomposite samples which are measured to further prove that the rGO thin-layers in LFP/rGO nanocomposites increase the material's electronic conductivity. According to the image, the Nyquist plots obtained are in the form of semicircles and slopes. The semicircle pattern in the high to medium frequency region shows the lithium ion charge-transfer process on the LFP/rGO and electrolyte surfaces. Meanwhile, the straight line (slopes) pattern in the lower frequency region represents the lithium ion diffusion process into the electrode bulk material, commonly known as Warburg diffusion. This pattern shows that the electrodes are capable of storing lithium ions, therefore suitable for use in lithium-ion batteries. The charge-transfer resistance width also determines the battery's electrical conductivity of the battery. An increase in pattern narrowness leads to an increase of its electrical conductivity. A comparison of the EIS profile semicircle diameters shows that the LFP/rGO nanocomposite cathode with a weight ratio of 70–30% (~ 350 ohm) has a much smaller charge-transfer resistance, compared to the counterpart with a ratio of 85–15% (~ 430 ohm). This much smaller solid-electrolyte interface resistance ought to be due to the rGO layers' presence in the LFP/rGO nanocomposite, with a much better electronic conductivity.

The galvanostatic charge–discharge (Fig. 8) was performed to evaluate LFP/rGO nanocomposite's electrochemical properties. The results obtained were as a graph of a relationship between the voltage and the charge–discharge capacity, provided with a constant current and a cut-off voltage of 2.5–4.2 volts during the analysis. Furthermore, the cutoff voltage is the initial voltage before treatment (charging and discharging). Lithium ions move from anode to

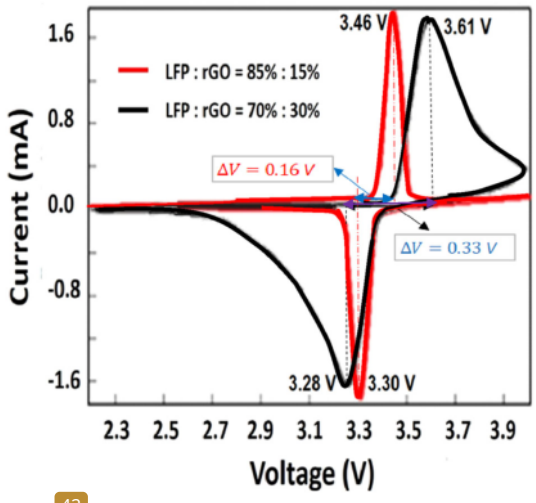

Fig. 6 The cyclic voltammetry curves of cathode material sample LFP/rGO nanocomposite at a ratio of 70–30% and 85–15%

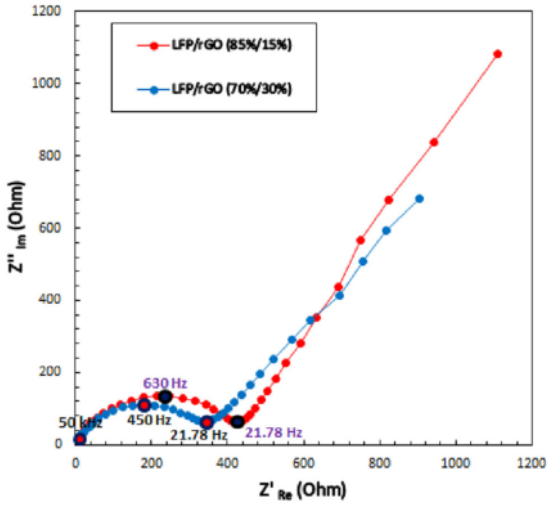

Fig. 7 Nyquist plots of LFP/rGO nanocomposite at a ratio of 70–30% and 85–15%

cathode until a maximum voltage of 4.2 volts is reached during charging. Subsequently, the ions move from cathode to anode until a minimum voltage of 2.5 volts is reached (discharging). There are flat plateaus of LFP/rGO nanocomposite from 3.4 V to 3.5 V that is exclusively for the transition of single phase of lithium iron phosphate to become iron-phosphate. According to the image, the first cycle's charge profile shows a stable voltage at 3.5 V (versus Li^+/Li) and this should be corresponding to the redox pair Fe^{2+}/Fe^{3+}. The discharge profile from the first cycle shows a stable voltage at 3.3 V (versus Li^+/Li) with a very small separation (0.2 V) being stable at the charge profile. The sample of LFP/rGO nanocomposite with ratio 85–15% shows the highest discharge capacity up to 128 $mAhg^{-1}$ and the lowest is showed by ratio 70–30% with discharge capacity 127 $mAhg^{-1}$. This excellent electrochemical performance is attributed to the large specific surface area and a wide bridging layer, ensuring electrons pass through each $LiFePO_4$ particle, shortening electronic transport pathways, and then reducing interface resistance. The lithium ions easily intercalate into the $LiFePO_4$ framework through the rGO layer and in turn avoids particle structure collapse during the charge shedding. Therefore, the LFP/rGO nanocomposite structure endures high current density charge/discharge. Figure 9 describes the performance of the LFP/rGO structure, with percentage ratios of 85:15 and 70:30, respectively, at rate 0.1 C. The graph displays that specific discharging average of both samples are 127.73 $mAhg^{-1}$ and 128.03 $mAhg^{-1}$ after 50 cycles. It shows a very well cyclic performance by retention capacities 97.73% and 97.75%. However, the LFP/rGO nanocomposite with ratio 85:15 obtained superior properties, compared to 70:30 on the level of 0.1 C. Furthermore, the sufficient stability of both samples without decreasing capacities denoted strong electrodes and stable solid electrolyte interfaces (SEI) as well as exhibited reversible kinetic reactions during cyclic reiteration.

4 Conclusion

Based on the overall results and discussions, an appropriate approach in synthesizing and characterizing the microstructure and electrochemical properties of rGO-based LFP cathode materials from old coconut shells has been proposed. LFP/rGO nanocomposites were successfully synthesized by combining the sol–gel route and mechanical ultracentrifugation techniques as an alternative to lithium ion battery cathode materials. The content of rGO prepared from biomass (old coconut shell) was varied between 15% and 30%. The results showed higher electrical conductivity and capacity as well as better cycle performance in LFP/rGO nanocomposites compared to pure LiFePO4 particles. Specific findings confirmed that the percentage ratio of synthesized LFP/rGO nanocomposite cathode (85:15) attained higher cycle capacity, compared to 70:30 on the level of 0.1 C, with specific discharging average of

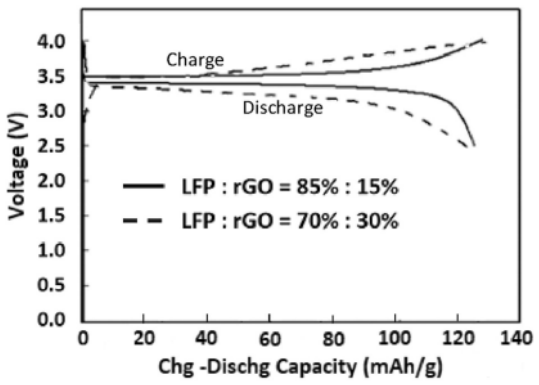

Fig. 8 Initial curve of charge and discharge of cathode material nanocomposite LFP/rGO sample at a ratio of 70–30% and 85–15%

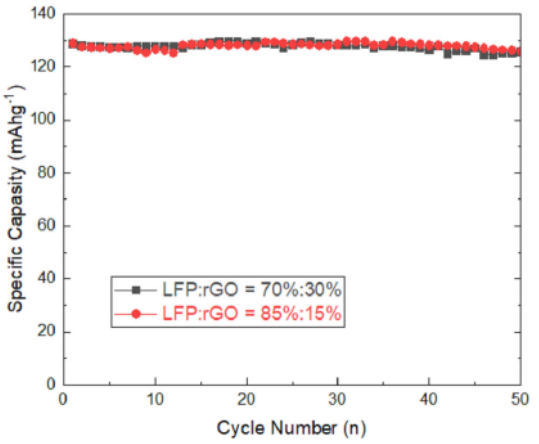

Fig. 9 Cycle life performance of the LFP/rGO at ratio of 70%:30% and the LFP/rGO at ratio of 18%:15% and was operated between 4.2 and 2.5 V at the current rate of 0.1 C

128.03 mAhg−1 and a retention capacity of 97.75% after 50 cycles, at room temperature and a rate of 0.1 C. The improved electrical conductivity and electrochemical performance of the prepared samples are believed to be done due to a three-dimensional conduction network provided by rGO-like carbon sheets as observed by electron microscopy. The findings in combination of the LFP and rGO nanoparticles drive maximum efficiency in their implementation. Moreover, the LFP particles are scattered and firmly attached to each rGO layer side, thus acting as a "bridge" among the LFP particles surroundings. The lithium ion has a greater diffusion distance between the crystal grain's boundary and its center due to larger crystal size. The rGO bridge is quite effective in limiting LFP grain growth as well as widening the surface area and shortening the lithium ions diffusion rate. In short, this work provides ideas in the utilization of biomass as a source of carbon compounds, including an rGO-like carbon, for technological applications of cathode materials for lithium ion batteries.

In the future with the same approach, it will be continued to synthesize another local green biomass and not only for lithium ion batteries but also will be developed for an alternative super-capacitor.

Acknowledgements

The authors would like to thank the Indonesian Endowment Fund for Education (LPDP) from the Indonesian Ministry of Finance for a full-ride scholarships through the BUDI-DN Doctorate program (ES) and PDUPT Research Grant (D) (20161141020723), 2021. We would also like to thank the Laboratory of Microelectronics and Laboratory of Institute of Nanoelectronics Engineering, University of Malaysia Perlis.

Declarations

Conflict of interest We authors declare that we do not have conflict of interest.

References

1. A.K. Padhi, K.S. Nanjundaswamy, J.B. Goodenough, J. Electrochem. Soc. **144**, 1188 (1997)
2. N.A. Hamid, S. Wennig, S. Hardt, A. Heinzel, C. Schulz, H. Wiggers, J. Power Sources **216**, 76 (2012)
3. C. Gong, Z. Xue, S. Wen, Y. Ye, X. Xie, J. Power Sources **318**, 93 (2016)
4. Z. Yu, L. Jiang, Solid State Ion. **325**, 12 (2018)
5. A. Eftekhari, J. Power Sources **17**, 393 (2017)
6. J. Ma, B. Li, H. Du, C. Xu, F. Kang, J. Solid State Electrochem. **16**, 1353 (2012)
7. X. Zhu, J. Hu, W. Wu, W. Zeng, H. Dai, Y. Du, Z. Liu, L. Li, H. Ji, Y. Zhu, J Mater Chem A **2**, 7812 (2014)
8. Y. Huang, H. Liu, L. Gong, Y. Hou, Q. Li, J. Power Sources **347**, 29 (2017)
9. L.N. Sun, Z.Y. Yuan, Y.F. Xue, W.L. Hong, X.Z. Ren, P.X. Zhang, Mater. Sci. Forum. **900**, 74 (2017)
10. Y. Liu, C. Cao, J. Li, Electrochim. Acta **55**, 3921 (2010)
11. H. Gong, H. Xue, T. Wang, J. He, J. Power Sources **318**, 220 (2016)
12. J. Wang, Ceram. Int. **40**, 6979 (2014)
13. A.Y. Nugraheni, M. Nasrullah, F.A. Prasetya, F. Astuti, Darminto, Mater. Sci. Forum **827**, 285 (2015)
14. M.K. Wardhani, F. Astuti, D. Darminto, J. Phys. Sci. Eng. **1**, 1 (2016)
15. R. Asih, E.B. Yutomo, D. Ristiani, M.A. Baqiya, T. Kawamata, M. Kato, I. Watanabe, Y. Koike, Darminto, Mater. Sci. Forum **966**, 290 (2019)
16. E.S.A. Serea, S.A. Mohamed, A.E. Shalan, M.M. Rashad, *Hybrid Perovskite Composite Materials* (Elsevier, Amsterdam, 2021), pp. 291–313
17. M.M. Moharam, A.N. El Shazly, K.V. Anand, D.E.-R.A. Rayan, M.K.A. Mohammed, M.M. Rashad, A.E. Shalan, Top. Curr. Chem. **379**, 20 (2021)
18. M.F. Sanad, A.E. Shalan, S.O. Abdellatif, E.S.A. Serea, M.S. Adly, Md.A. Ahsan, Top. Curr. Chem. **378**, 48 (2020)
19. A.E. Shalan, N. Perinka, E.S.A. Serea, M.F. Sanad, *Advanced Lightweight Multifunctional Materials* (Elsevier, UK, 2021), p. 153
20. K. Valadi, S. Gharibi, R. Taheri-Ledari, S. Akin, A. Maleki, A.E. Shalan, Environ. Chem. Lett. **19**, 2185 (2021)
21. A.E. Shalan, M.K.A. Mohammed, N. Govindan, RSC Adv. **11**, 4417 (2021)
22. S.M. Abdelbasir, A.E. Shalan, Korean J. Chem. Eng. **36**, 1209 (2019)
23. S.N. Alam, N. Sharma, L. Kumar, Graphene **06**, 1 (2017)
24. P. Russo, A. Hu, G. Compagnini, Nano-Micro Lett. **5**, 260 (2013)
25. H. Bi, F. Huang, Y. Tang, Z. Liu, T. Lin, J. Chen, W. Zhao, Electrochim. Acta **88**, 414 (2013)
26. M.T.H. Aunkor, I.M. Mahbubul, R. Saidur, H.S.C. Metselaar, RSC Adv. **6**, 27807 (2016)
27. F. Iskandar, Y. Rus, Adv. Mater. Res. **1112**, 290 (2015)

28. M. Chen, K. Kou, M. Tu, J. Hu, X. Du, B. Yang, Solid State Ion. **310**, 95 (2017)
29. W. Song, J. Liu, L. You, S. Wang, Q. Zhou, Y. Gao, R. Yin, W. Xu, Z. Guo, J. Power Sources **419**, 192 (2019)
30. J. Liu, X. Lin, T. Han, X. Li, C. Gu, J. Li, Appl. Surf. Sci. **459**, 233 (2018)
31. A.V. Murugan, T. Muraliganth, A. Manthiram, J. Phys. Chem. C **112**, 14665 (2008)
32. W. Shang, L. Kong, X. Ji, Solid State Sci. **38**, 79 (2014)
33. Z. Yuan, Y. Xue, L. Sun, Y. Li, H. Mi, L. Deng, W. Hong, X. Ren, P. Zhang, Ferroelectrics **528**, 1 (2018)
34. K.S. Dhindsa, B.P. Mandal, K. Bazzi, M.W. Lin, M. Nazri, G.A. Nazri, V.M. Naik, V.K. Garg, A.C. Oliveira, P. Vaishnava, R. Naik, Z.X. Zhou, Solid State Ion. **253**, 94 (2013)
35. G. Yuan, J. Bai, T.N.L. Doan, P. Chen, Mater. Lett. **158**, 248 (2015)
36. R. Wang, C. Xu, J. Sun, L. Gao, J. Jin, C. Lin, Mater. Lett. **112**, 207 (2013)
37. C. Su, X. Bu, L. Xu, J. Liu, C. Zhang, Electrochim. Acta **64**, 190 (2012)
38. X. Lei, H. Zhang, Y. Chen, W. Wang, Y. Ye, C. Zheng, P. Deng, Z. Shi, J. Alloys Compd. **626**, 280 (2015)
39. Z. Tian, S. Liu, F. Ye, S. Yao, Z. Zhou, S. Wang, Appl. Surf. Sci. **305**, 427 (2014)
40. Y. Ding, Y. Jiang, F. Xu, J. Yin, H. Ren, Q. Zhuo, Z. Long, P. Zhang, Electrochem. Commun. **12**, 10 (2010)
41. S.H. Ha, Y.J. Lee, Chem Eur J. **20**, 1 (2014)
42. C.H.A. Tsang, H. Huang, J. Xuan, H. Wang, D.Y.C. Leung, Renew. Sustain. Energy Rev. **120**, 1 (2020)
43. Z. Bo, X. Shuai, S. Mao, H. Yang, J. Qian, J. Chen, J. Yan, K. Cen, Sci. Rep. **4**, 4684 (2015)
44. J. Wang, E.C. Salihi, L. Šiller, Mater. Sci. Eng. C **72**, 1 (2017)
45. J. Jagiełło, A. Chlanda, M. Baran, M. Gwiazda, L. Lipińska, Nanomaterials **10**, 1846 (2020)
46. E. Suarso, A.Z. Laila, F.A. Setyawan, M. Zainuri, Z. Arifin, Darminto, Mater. Sci. Forum **966**, 386 (2019)
47. R. Angela, H. Islam, V. Sari, C. Latif, M. Zainuri, and S. Pratapa, in (Solo, Indonesia, 2017), p. 030102.
48. N. Elgrishi, K.J. Rountree, B.D. McCarthy, E.S. Rountree, T.T. Eisenhart, J.L. Dempsey, J. Chem. Educ. **95**, 197 (2018)

Terms and Conditions

Springer Nature journal content, brought to you courtesy of Springer Nature Customer Service Center GmbH (“Springer Nature”).

Springer Nature supports a reasonable amount of sharing of research papers by authors, subscribers and authorised users (“Users”), for small-scale personal, non-commercial use provided that all copyright, trade and service marks and other proprietary notices are maintained. By accessing, sharing, receiving or otherwise using the Springer Nature journal content you agree to these terms of use (“Terms”). For these purposes, Springer Nature considers academic use (by researchers and students) to be non-commercial.

These Terms are supplementary and will apply in addition to any applicable website terms and conditions, a relevant site licence or a personal subscription. These Terms will prevail over any conflict or ambiguity with regards to the relevant terms, a site licence or a personal subscription (to the extent of the conflict or ambiguity only). For Creative Commons-licensed articles, the terms of the Creative Commons license used will apply.

We collect and use personal data to provide access to the Springer Nature journal content. We may also use these personal data internally within ResearchGate and Springer Nature and as agreed share it, in an anonymised way, for purposes of tracking, analysis and reporting. We will not otherwise disclose your personal data outside the ResearchGate or the Springer Nature group of companies unless we have your permission as detailed in the Privacy Policy.

While Users may use the Springer Nature journal content for small scale, personal non-commercial use, it is important to note that Users may not:

1. use such content for the purpose of providing other users with access on a regular or large scale basis or as a means to circumvent access control;
2. use such content where to do so would be considered a criminal or statutory offence in any jurisdiction, or gives rise to civil liability, or is otherwise unlawful;
3. falsely or misleadingly imply or suggest endorsement, approval , sponsorship, or association unless explicitly agreed to by Springer Nature in writing;
4. use bots or other automated methods to access the content or redirect messages
5. override any security feature or exclusionary protocol; or
6. share the content in order to create substitute for Springer Nature products or services or a systematic database of Springer Nature journal content.

In line with the restriction against commercial use, Springer Nature does not permit the creation of a product or service that creates revenue, royalties, rent or income from our content or its inclusion as part of a paid for service or for other commercial gain. Springer Nature journal content cannot be used for inter-library loans and librarians may not upload Springer Nature journal content on a large scale into their, or any other, institutional repository.

These terms of use are reviewed regularly and may be amended at any time. Springer Nature is not obligated to publish any information or content on this website and may remove it or features or functionality at our sole discretion, at any time with or without notice. Springer Nature may revoke this licence to you at any time and remove access to any copies of the Springer Nature journal content which have been saved.

To the fullest extent permitted by law, Springer Nature makes no warranties, representations or guarantees to Users, either express or implied with respect to the Springer nature journal content and all parties disclaim and waive any implied warranties or warranties imposed by law, including merchantability or fitness for any particular purpose.

Please note that these rights do not automatically extend to content, data or other material published by Springer Nature that may be licensed from third parties.

If you would like to use or distribute our Springer Nature journal content to a wider audience or on a regular basis or in any other manner not expressly permitted by these Terms, please contact Springer Nature at

onlineservice@springernature.com

Eka Suarso _ Enhancement of LiFePO4 (LFP) electrochemical performance through the insertion of coconut shellderived rGO-like carbon as cathode of Li-ion battery

ORIGINALITY REPORT

15%	5%	15%	1%
SIMILARITY INDEX	INTERNET SOURCES	PUBLICATIONS	STUDENT PAPERS

PRIMARY SOURCES

1	Xiaoling Ma, Gongxuan Chen, Qiong Liu, Guoping Zeng, Tian Wu. " Synthesis of LiFePO /Graphene Nanocomposite and Its Electrochemical Properties as Cathode Material for Li-Ion Batteries ", Journal of Nanomaterials, 2015 Publication	3%
2	Eka Suarso, Anna Zakiyatul Laila, Firsta Agung Setyawan, Mochamad Zainuri, Zaenal Arifin, Darminto. "The Effect of Reduced Graphene Oxide (rGO) Coating on Electrical Conductivity of Lithium Ferro Phosphate (LFP) as an Alternative Cathode for Li-Ion Battery", Materials Science Forum, 2019 Publication	2%
3	Waqas Ahmad, Zaka Ullah, Nazmina Imrose Sonil, Karim Khan. "Introduction, production, characterization and applications of defects in graphene", Journal of Materials Science: Materials in Electronics, 2021	1%

	Publication	
4	kb.psu.ac.th:8080 Internet Source	1 %
5	apsacollege.com Internet Source	1 %
6	ejournal.umm.ac.id Internet Source	<1 %
7	onlinelibrary.wiley.com Internet Source	<1 %
8	www.scientific.net Internet Source	<1 %
9	In-Chul Kim, Dongjin Byun, Joong Kee Lee. "Electrochemical characteristics of silicon-metals coated graphites for anode materials of lithium secondary batteries", Journal of Electroceramics, 2006 Publication	<1 %
10	M. Stanley Whittingham. "Lithium Batteries and Cathode Materials", Chemical Reviews, 2004 Publication	<1 %
11	daneshyari.com Internet Source	<1 %
12	jecst.org Internet Source	<1 %

13	Dae-wook Kim, Nobuyuki Zettsu, Katsuya Teshima. "Three-Dimensional Electric Micro-Grid Network for High-Energy-Density Lithium-Ion Battery Cathodes", J. Mater. Chem. A, 2017 Publication	<1 %
14	Liping He, Wenke Zha, Dachuan Chen. " Crystal growth kinetics, microstructure and electrochemical properties of LiFePO /carbon nanocomposites fabricated using a chelating structure phosphorus source ", RSC Advances, 2018 Publication	<1 %
15	Tan Ji Siang, Long Giang Bach, Sharanjit Singh, Quang Duc Truong et al. "Methane bi-reforming over boron-doped Ni/SBA-15 catalyst: Longevity evaluation", International Journal of Hydrogen Energy, 2019 Publication	<1 %
16	www2.mdpi.com Internet Source	<1 %
17	Liangliang Gao, Yi Jin, Xiaofang Liu, Ming Xu, Xiaokang Lai, Jianglan Shui. "A rationally assembled graphene nanoribbon/graphene framework for high volumetric energy and power density Li-ion batteries", Nanoscale, 2018 Publication	<1 %

18	mafiadoc.com Internet Source	<1%
19	www.biyanicolleges.org Internet Source	<1%
20	Sabah Mohamed Abdelbasir, Ahmed Esmail Shalan. "An overview of nanomaterials for industrial wastewater treatment", Korean Journal of Chemical Engineering, 2019 Publication	<1%
21	Swapnil J. Rajoba, Lata D. Jadhav, Ramchandra S. Kalubarme, Pramod S. Patil, S. Varma, B.N. Wani. "Electrochemical performance of LiFePO 4 /GO composite for Li-ion batteries", Ceramics International, 2018 Publication	<1%
22	Wen-Chen Chien, Kung-Nan Liu, Shih-Chang Chang, Chun-Chen Yang. "Effects of α-Fe 2 O 3 size and morphology on performance of LiFePO 4 /C cathodes for Li-ion batteries", Thin Solid Films, 2018 Publication	<1%
23	Zhe Tian, Zhufa Zhou, Shanshan Liu, Feng Ye, Sijia Yao. "Enhanced properties of olivine LiFePO 4 /graphene co-doped with Nb 5+ and Ti 4+ by a sol–gel method", Solid State Ionics, 2015 Publication	<1%

24	Zhiqiang Lv, Moxiang Ling, Meng Yue, Xianfeng Li, Mingming Song, Qiong Zheng, Huamin Zhang. "Vanadium-based polyanionic compounds as cathode materials for sodium-ion batteries: toward high-energy and high-power applications", Journal of Energy Chemistry, 2020 Publication	<1 %
25	Houbin Liu, Cui Miao, Yan Meng, Yan-Bing He, Qiang Xu, Xinhe Zhang, Zhiyuan Tang. "Optimized synthesis of nano-sized LiFePO4/C particles with excellent rate capability for lithium ion batteries", Electrochimica Acta, 2014 Publication	<1 %
26	Hu, Yemin, Genhui Wang, Chenzi Liu, Shu-Lei Chou, Mingyuan Zhu, Hongming Jin, Wenxian Li, and Ying Li. "LiFePO4/C nanocomposite synthesized by a novel carbothermal reduction method and its electrochemical performance", Ceramics International, 2016. Publication	<1 %
27	Jun Xia, Fuliang Zhu, Gongrui Wang, Lei Wang, Yanshuang Meng, Yue Zhang. "Synthesis of LiFePO 4 /C using ionic liquid as carbon source for lithium ion batteries", Solid State Ionics, 2017 Publication	<1 %

28	Pola, J.. "Megawatt laser photolysis of trimethyl(vinyloxy)silane: formation of nano-sized cross-linked polyoxocarbosilane with superior thermal stability", Journal of Non-Crystalline Solids, 20031015 Publication	<1 %
29	Quanyi Hao, Danni Lei, Xiaoming Yin, Ming Zhang, Shuang Liu, Qiuhong Li, Libao Chen, Taihong Wang. "3-D mesoporous nano/micro-structured Fe3O4/C as a superior anode material for lithium-ion batteries", Journal of Solid State Electrochemistry, 2010 Publication	<1 %
30	Syed Fariq Fathullah Syed Yaacob, Muhammad Afzal Kamboh, Wan Aini Wan Ibrahim, Sharifah Mohamad. "New sporopollenin-based β-cyclodextrin functionalized magnetic hybrid adsorbent for magnetic solid-phase extraction of nonsteroidal anti-inflammatory drugs from water samples", Royal Society Open Science, 2018 Publication	<1 %
31	Wu, Songping, Rui Xu, Mingjia Lu, Rongyun Ge, James Iocozzia, Cuiping Han, Beibei Jiang, and Zhiqun Lin. "Graphene-Containing Nanomaterials for Lithium-Ion Batteries", Advanced Energy Materials, 2015.	<1 %

Publication

32	Zhihao Yu, Linhua Jiang. "Olivine LiFePO 4 nanocrystals grown on nitrogen-doped graphene sheets as high-rate cathode for lithium-ion batteries", Solid State Ionics, 2018 Publication	<1 %
33	tnsroindia.org.in Internet Source	<1 %
34	A. Amali Roselin, R. Karkuzhali, N. Anandhan, G. Gopu. "Bismuth titanate (Bi4Ti3O12, BTO) sol–gel spin coated thin film for heavy metal ion detection", Journal of Materials Science: Materials in Electronics, 2021 Publication	<1 %
35	Ali Eftekhari. "LiFePO 4 /C nanocomposites for lithium-ion batteries", Journal of Power Sources, 2017 Publication	<1 %
36	Boya Wang, Lei Yao, Yan Wang, Jinhua Wu, Qiong Wang, Mingwu Xiang, Yun Zhang, Hao Wu, Heng Liu. "Synthesis of Porous Bowl-like LiFePO4/C Composite with Ultrahigh Rate Capability", International Journal of Electrochemical Science, 2017 Publication	<1 %
37	Chaironi Latif, Anisa Fitri Muyasaroh, Amalia Firdausi, Dina Mardiana et al. "Preparation	<1 %

and characterisation of LiFePO4 ceramic powders via dissolution method", Ceramics International, 2021
Publication

---

38 Chunli Gong, Zhigang Xue, Sheng Wen, Yunsheng Ye, Xiaolin Xie. "Advanced carbon materials/olivine LiFePO 4 composites cathode for lithium ion batteries", Journal of Power Sources, 2016 <1%
Publication

---

39 Karuppiah, Saravanan, Suganya Vellingiri, and Kalaiselvi Nallathamby. "Newer polyanionic bio-composite anode for sodium ion batteries", Journal of Power Sources, 2017. <1%
Publication

---

40 Malik Anjelh Baqiya, Ananda Yogi Nugraheni, Wildatun Islamiyah, Affandi Faisal Kurniawan et al. "Structural study on graphene-based particles prepared from old coconut shell by acid–assisted mechanical exfoliation", Advanced Powder Technology, 2020 <1%
Publication

---

41 research-repository.griffith.edu.au <1%
Internet Source

---

42 Saroha, Rakesh, Amrish K. Panwar, Yogesh Sharma, Pawan K. Tyagi, and Sudipto Ghosh. "Development of surface functionalized ZnO-doped LiFePO4/C composites as alternative <1%

cathode material for lithium ion batteries", Applied Surface Science, 2017.
Publication

Exclude quotes	Off	Exclude matches	Off
Exclude bibliography	On		

Eka Suarso _ Enhancement of LiFePO4 (LFP) electrochemical performance through the insertion of coconut shellderived rGO-like carbon as cathode of Li-ion battery

GRADEMARK REPORT

FINAL GRADE

/100

GENERAL COMMENTS

PAGE 1

PAGE 2

PAGE 3

PAGE 4

PAGE 5

PAGE 6

PAGE 7

PAGE 8

PAGE 9

PAGE 10

PAGE 11